

Comparison of the Spherical Deflector and the Cylindrical Mirror Analyzers

H. Hafner, J. Arol Simpson, and C. E. Kuyatt

Citation: *Rev. Sci. Instrum.* **39**, 33 (1968); doi: 10.1063/1.1683103

View online: <http://dx.doi.org/10.1063/1.1683103>

View Table of Contents: <http://rsi.aip.org/resource/1/RSINAK/v39/i1>

Published by the [American Institute of Physics](#).

Additional information on *Rev. Sci. Instrum.*

Journal Homepage: <http://rsi.aip.org>

Journal Information: http://rsi.aip.org/about/about_the_journal

Top downloads: http://rsi.aip.org/features/most_downloaded

Information for Authors: <http://rsi.aip.org/authors>

ADVERTISEMENT

**AIP**Advances

Submit Now

**Explore AIP's new
open-access journal**

- **Article-level metrics
now available**
- **Join the conversation!
Rate & comment on articles**

Comparison of the Spherical Deflector and the Cylindrical Mirror Analyzers

H. HAFNER,* J. AROL SIMPSON, AND C. E. KUYATT

National Bureau of Standards, Washington, D. C. 20234

(Received 18 August 1967; and in final form, 19 September 1967)

The calculated performance of electrostatic analyzers of the cylindrical and spherical deflection type are compared. It is shown that considering geometrical terms through the third order the cylindrical device is significantly superior.

FOR many years the concentric spherical deflection analyzer as described by Purcell¹ has been the best electrostatic analyzer known, the reduced dispersion (dispersion/aberration constant) being larger than either that of the concentric cylindrical deflection device² or the parallel plate mirror analyzer.³ Furthermore, the spherical deflection system provides two-dimensional focusing as an additional advantage in devices using axially symmetric beams. Recently, Zashkvara *et al.*⁴ have shown that the cylindrical mirror analyzer used by Blauth⁵ has the unsuspected property that second order focusing occurs at $\alpha_0 = 42.3^\circ$ and $E_0/eV = 1.3/\ln r_2/r_1$ where V is the potential difference between the two concentric cylinders (radius r_1 and r_2) and E_0 is the kinetic energy of a particle with charge e emitted by a point source S on the axis of rotation (Fig. 1). Refocusing occurs at $L_0 = 6.1r_1$ and the maximum distance off axis is $r_m = 1.8r_1$.

The Taylor series for $\Delta L = L - L_0$, $\Delta L = f(\Delta E, \Delta\alpha)$ with $\Delta E = E - E_0$ and $\Delta\alpha = \alpha - \alpha_0$ is⁴

$$\Delta L = 5.6r_1(\Delta E/E_0) - 15.4r_1(\Delta\alpha)^3 + 10.3r_1(\Delta E/E_0)\Delta\alpha. \quad (1)$$

Other terms appear in higher order either of ΔE or $\Delta\alpha$ or both and with coefficients too small to make their contribution noticeable. In order to estimate the influence of the third term in Eq. (1), we assume that the analyzer will be designed according to established procedures⁶ which require the second term of Eq. (1) to be about one half of the dispersion term. With this choice, the third term will be about 30% of the dispersion term at $\Delta\alpha = 10^\circ$. This may indicate that the contribution of the third term in Eq. (1) will in general not be negligible. However, the contribution of this term is symmetrical in $\Delta\alpha$ to the $\Delta\alpha = 0$ ray. The half width of the transmission function of such an analyzer will therefore not be significantly changed if this term is taken into account, although a considerable broadening of the base width occurs. For example, at $\Delta\alpha = 10^\circ$ and an exit slit width equal to the trace width due to the $(\Delta\alpha)^3$ term, the transmission function will be

* Guest Worker from Physikalisches Institut, Universität Tübingen, supported by NATO.

¹ E. M. Purcell, Phys. Rev. **54**, 818 (1938).

² A. L. Hughes and V. Rojansky, Phys. Rev. **34**, 284 (1929).

³ G. A. Harrower, Rev. Sci. Instr. **26**, 850 (1955).

⁴ V. V. Zashkvara, M. I. Korsunskii, O. S. Kosmachev, Soviet Phys.-Tech. Phys. (English Transl.) **11**, 96 (1966).

⁵ E. Blauth, Z. Physik **147**, 228 (1951).

⁶ C. E. Kuyatt and J. Arol Simpson, Rev. Sci. Instr. **38**, 103 (1967).

broadened at its base by about 25%, the half width remaining unchanged.

The reduced dispersion of the cylindrical mirror analyzer may, therefore, be described in a sufficiently significant manner by the constants of linear dispersion and the $(\Delta\alpha)^3$ aberration term.

Since the focus of the cylindrical mirror is of higher order than that of the spherical deflector, a comparison of reduced dispersion cannot be made. However, a comparison of resolving power as a function of angle is worthwhile, since the cylindrical mirror analyzer offers several advantages. Since the beam enters through an equipotential surface, in the actual performance it will be easy to correct the fringe field of the entrance slit. Furthermore, the extension of collecting angle in the rotation plane is simple.

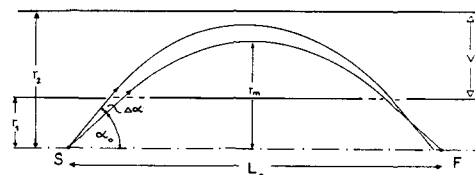


FIG. 1. Electron trajectories in the cylindrical mirror. S—source; F—focus.

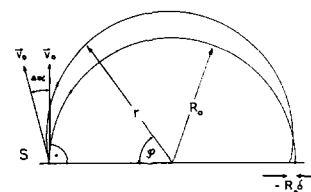


FIG. 2. Electron trajectories in the 180° spherical deflector

In order to obtain the angular range where the higher order focus of the cylindrical mirror analyzer is an additional advantage, the higher order terms of the spherical analyzer are required. The third order aberration coefficient of the spherical deflection analyzer will be derived for the 180° device which is most often used. We assume a point source at the entrance plane of the analyzer emitting monoenergetic electrons with velocity v_0 and angles $\Delta\alpha$ relative to the direction perpendicular to the entrance plane as shown in Fig. 2.

The differential equations in a central force field are

$$\begin{aligned} \ddot{r} + (e/m)(C_1/r^2) - r\dot{\varphi}^2 &= 0, \\ (d/dt)(mr^2\dot{\varphi}) &= 0, \end{aligned}$$

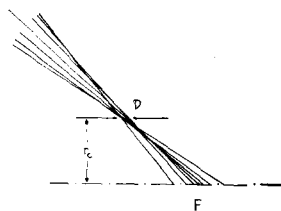


FIG. 3. Dimension D and position r_0 of minimum trace width. D is measured parallel to the axis.

where m is the electron mass and C_1 describes the field strength as a function of both the potential difference between the two spherical surfaces of the analyzer and their radii. C_1 is not a function of coordinates φ , r . The solutions are

$$\begin{aligned} 1/r &= A \sin \varphi + B \cos \varphi + (C_1/C_2^2)(e/m) \\ C_2 &= r^2 \dot{\varphi}, \end{aligned}$$

where C_2 is the angular momentum, which is a constant of motion in a $1/r^2$ -field of force. C_2 may be obtained by setting $\varphi=0$. Then we have $v=v_0$, $r=R_0$, and

$$C_2 = r^2 \dot{\varphi} = R_0 v_0 \cos \Delta\alpha.$$

A and B are integration constants. In order to obtain B (A will not be necessary in this case where φ scans 180°), we adjust C_1 so that the electron starting at S with $\alpha=0$ travels along a circle with radius R_0 . This requires

$$e(C_1/R_0^2) = e |f(R_0)| = m(v_0^2/R_0).$$

Here $f(R_0)$ is the electric field strength at R_0 . This yields

$$C_1 = (m/e)R_0 v_0^2,$$

hence at

$$\varphi=0, \quad r=R_0; \quad B = (1/R_0) - (1/R_0 \cos^2 \Delta\alpha).$$

At $\varphi=180^\circ$, the equation of motion yields

$$1/R_0(1+\delta) = -(1/R_0) + (2/R_0 \cos^2 \Delta\alpha)$$

or

$$R_0(1+\delta) = R_0 \cos^2 \Delta\alpha / (2 - \cos^2 \Delta\alpha) = R_0 \cos^2 \Delta\alpha / (1 + \sin^2 \Delta\alpha)$$

for the position of the electron in the exit plane, where $R_0\delta$ is the displacement caused by $\Delta\alpha$. Using the approxi-

TABLE I. Properties of the cylindrical mirror analyzer.

$\Delta\alpha^\circ$	6	8	10	12	14	16
Full trace width $2\Delta L \cdot (10^2/r_1)$	3.5	8.3	16	28	45	68
Trace width Dispersion $\cdot 10^2$	0.63	1.5	2.9	5.0	8.1	12
Minimum trace width $D \cdot (10^2/r_1)$	0.88	2.3	4.5	8.1	13	21
Position $(r_e/r_1) \cdot 10$	0.83	1.1	1.7	2.4	3.3	4.4
Trace width at image Minimum trace width	4	3.7	3.6	3.5	3.4	3.2

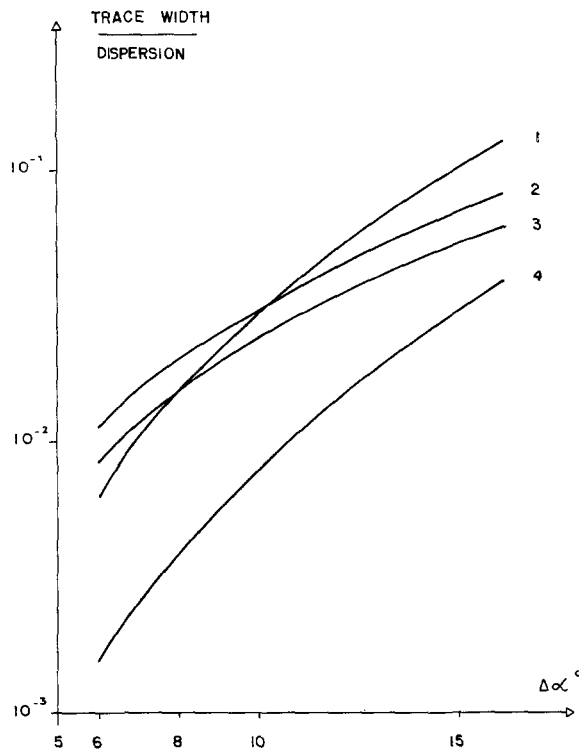


FIG. 4. Reduced aberration of cylindrical mirror and spherical deflector as a function of half angle of the incident beam. 1—Cylindrical mirror, exit slit at image; 2— 180° spherical deflector; 3—optimum sphere; and 4—cylindrical mirror, exit slit at plane of minimum trace width.

mation

$$1/(1 + \sin^2 \Delta\alpha) = 1 - \sin^2 \Delta\alpha,$$

in which the first term neglected is of fourth order in $\Delta\alpha$, we obtain

$$R_0(1+\delta) = R_0 \cos^4 \Delta\alpha$$

or, with

$$\cos \Delta\alpha = 1 - [(\Delta\alpha)^2/2],$$

we finally obtain in the third order approximation

$$\delta = -2(\Delta\alpha)^2.$$

Hence, the third order term vanishes.

In order to compare the two analyzers, it is necessary to take into account the difference in focusing. The second order term of the spherical analyzer produces an image of the point source with a trace width $2(\Delta\alpha)^2 R_0$ measured in the exit plane, focusing paths with $-\Delta\alpha$ and $+\Delta\alpha$ at the same point. The third order term of the cylindrical mirror causes a trace width of $2 \times 15.4 r_1 (\Delta\alpha)^3$, because paths with $-\Delta\alpha$ are displaced by the same amount, but in opposite directions from the focus F .

The linear dispersion constant of the spherical deflector is $2R_0$, and the ratio of trace width to dispersion is $(\Delta\alpha)^2$. The corresponding value for the cylindrical mirror is $2 \cdot (15.4/5.6) (\Delta\alpha)^3$. This means, that at half angles

$$\Delta\alpha < 0.18,$$

the cylindrical mirror analyzer yields a higher resolving power than the spherical deflector operated at the same $\Delta\alpha$.

It is well known in light optics that in the presence of an odd order aberration there exists a plane different from the image plane where the trace width is a minimum.⁷ The negative sign of the aberration coefficient indicates that this plane lies before the axial image of the cylindrical mirror. This is an additional advantage of the device. As the minimum trace width occurs before the image, the aperturing of the exit beam is simplified, especially in the case where the collecting angle in the plane perpendicular to the axis of rotation is extended to 2π . Furthermore, by positioning the exit slit at the minimum trace width rather than at the first order image, the resolving power is increased considerably. The relevant quantities for the angular range of $\Delta\alpha=6^\circ \dots 16^\circ$ are shown in Table I. Angles higher than 16° are of less interest because the resolution of the device, even if operated at very low energy, would exceed the energy distribution width of an electron beam created by an oxide cathode. The figures concerned with minimum trace width have been obtained graphically. D and r_c are defined in Fig. 3.

In Fig. 4, the reduced aberration (trace width/dispersion) of the cylindrical mirror analyzer with the slit at the image plane and also with the slit at the plane of minimum trace width is plotted together with the same property of

⁷ A. E. Conrady, *Applied Optics and Optical Design* (Dover Publications, Inc., New York, 1957), p. 120 *et seq.*

the 180° spherical analyzer and of the spherical analyzer in its optimum configuration where the reduced dispersion is a maximum. (According to Purcell,¹ the reduced dispersion is a maximum for a spherical sector operated with an image distance from the center which is twice the source distance from this point.) Figure 4 shows that, at the larger values of $\Delta\alpha$ of practical interest, the optimum cylindrical mirror analyzer is superior to the spherical deflection analyzer even in its optimum configuration.

A numerical example illustrates the advantage of the cylindrical mirror. With a point source and $\Delta\alpha=10^\circ$, a full width at half maximum of the energy distribution of an analyzer beam of $\Delta E_{\frac{1}{2}}=9\times 10^{-3}E_0$ can be obtained. The high value of $\Delta\alpha$ of course means, that at the same $\Delta E_{\frac{1}{2}}$ the cylindrical mirror will provide a higher current of analyzed particles than the spherical deflector.

The figures given are superior to any previously available and should lead to analyzers of significantly better performance than previously available, although there remains the problem of designing lenses which operate at the large angles required by the cylindrical mirror analyzer.

Note added in proof. Since this manuscript was submitted, H. Z. Sar-el, *Rev. Sci. Instr.* **38**, 1210 (1967), published a more extensive analysis of the cylindrical mirror analyzer than that of Zashkvara *et al.*,⁴ and described the construction and performance of a prototype instrument. Sar-el's extension of the theory is not needed for our treatment.

Gauge for Measuring Impulsive Pressure in a Container Subjected to Large, Time-Varying Applied Voltages*

W. R. GRABOWSKY AND D. A. DURRAN

Aerospace Corporation, El Segundo, California 90045

(Received 13 July 1966; and in final form, 2 October 1967)

A pressure gauge consisting of a strain-gauge transducer, bridge, and decoupler is described for the measurement of time-varying pressures in the presence of an electrical noise environment typical of capacitor discharge systems. In particular, the transducer of the gauge has been subjected to large, time-varying applied voltages,

$$V_{\max} \approx 10^8 \text{ V and } [(dv/dt)]_{\max} \approx 5 \times 10^6 \text{ V/sec,}$$

and large, time-varying magnetic fields,

$$B_{\max} \approx 2 \times 10^4 \text{ G and } [(dB/dt)]_{\max} \approx 5 \times 10^6 \text{ G/sec,}$$

with no ill effect on the output of the gauge. At least an order of magnitude increase in these quantities (i.e., V_{\max} , etc.) is believed possible without serious effect on the gauge output. The gauge can be statically calibrated, has a rise time of $\sim 4 \mu\text{sec}$, and can be compensated for electronic drift.

I. INTRODUCTION

COMMERCIAL instrumentation for the electrical readout of an impulsively generated gaseous pressure is accurate and reliable, provided that the elec-

trical potential of the pressure transducer remains the same as that of the readout equipment throughout the time of measurement. In certain experiments it may be impractical, if not impossible, to maintain a balanced potential between the transducer and the readout equipment. In such experiments the measure-

* Supported by the U. S. Air Force under Contract No. AF 04(695)-1001.